were generated and digitized. The H&E sections were registered to the MRI with a registration-error less than 3 mm. Spearman's correlation between tumor ADC and micro anatomical variables were calculated using an automatic pixel counting algorithm (AperioTechnologies) (Figure 1).

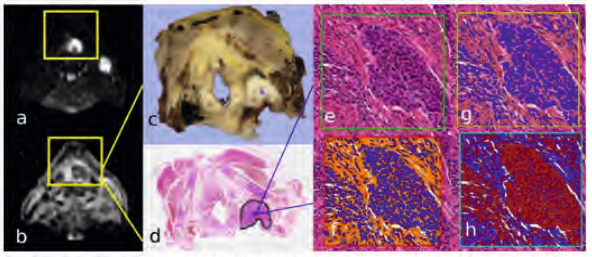

Figure 1. Registered diffusion weighted imaging with pathology and histology of a patient with a hypopharyngeal tumor. The ADC map (b) with b800 DWI (a) and the corresponding pathological slice (c) and whole mount digitized HE section (d) all show the tumor. The HE section was digitized at histological resolution, enabling color based segmentation. Nuclear density (g), regarded as cell density, percentage areas of nuclei (blue, f), cytoplasm ((red, h)-(blue, f)) and stroma (blue, h), and nuclear-to-cytoplasmic ratio (N/C) within the tumor were determined using color based segmentation on four consecutive slices.

Results: ADC was significantly and inversely correlated to cell density, percentage area of nuclei and N/C ratio. ADC was significantly and positively related to percentage area of stroma. Additionally, the percentage area of stroma was strongly interdependent with the percentage area of nuclei (Table 1).

TABLE 1. Microanatomical parameters and correlation with ADC

	CD (n=16)	% nuclei (n=12)	% cytoplasm (n=12)	% stroma (n=12)	N/C ratio (n=12)
Mean (range)	6406 (4806-8050)	43.1 (24.1-70.2)	19.6 (11.2-27.1)	39.6 (14.0-75.8)	2.4 (1.1-4.7)
Correlation ADC r (P value)	- 0.57 (0.02)	-0.66 (0.02)	0.45 (0.15)	0.68 (0.02)	- 0.78 (<0.01)
Correlation % nuclei r (P value)	-	1.000	- 0.01 (0.97)	- 0.97 (<0.01)	0.64 (0.03)

Conclusions: ADC was significantly correlated with cellularity, stromal component and the nuclear-to-cytoplasm ratio. These results give us insights into how ADC reflects the underlying microanatomical environment. The correlation between stromal component, a known predictor of local failure, and ADC might suggest that the poor prognostic value of a high pre-treatment ADC might partly be attributed to the tumor-stroma component.

[1]Hakatenaka et al, Int J Radiat Oncol Biol Phys. 2011

OC-0148

Characterization of vasculature in NSCLC tumours using perfusion CT and FDG-PET/CT imaging

W. van Elmpt[1], M. Das[2], H. Sharifi[1], C. Zegers[1], M. Öllers[1], J. Wildberger[2], D. De Ruysscher[1]
[1]*Maastricht University Medical Centre, Department of Radiation Oncology (MAASTRO), Maastricht, The Netherlands*
[2]*Maastricht University Medical Centre, Department of Radiology, Maastricht, The Netherlands*

Purpose/Objective: Dynamic contrast enhanced CT imaging ('perfusion CT') is a technique for the quantification of vasculature inside tumours. If combined with FDG-PET/CT imaging a more complete assessment of the tumour heterogeneity is possible. In this study we investigated non-small cell lung cancer (NSCLC) patients undergoing both techniques on the same day to quantify the correlation of vasculature properties with metabolically active regions.
Materials and Methods: A total of 12 patients diagnosed with stage II-III NSCLC were analysed from two ongoing clinical trials (NCT01024829 and NCT01210378) prior to (chemo-)radiotherapy treatment were scheduled for FDG-PET/CT (Siemens Biograph 40 PET/CT) and perfusion CT (Siemens Definition Flash CT) imaging. The primary gross tumour volume (GTV) was delineated on the PET/CT scan for treatment planning purposes. Datasets of both imaging modalities (FDG-PET/CT and perfusion CT) were registered and metabolic uptake regions on the FDG-PET/CT were thresholded in 2 regions inside the GTV: a low (0-50% of the maximum SUV) and high metabolic uptake (>50% of the maximum SUV). Commercial perfusion CT software (Siemens VPCT; deconvolution algorithm approach) was used to extract inside the 2 thresholded regions the vasculature properties op the tumour: blood flow (BF), blood volume (BV), permeability (PMB) and mean transit time (MTT). Differences in vasculature between low and high uptake volumes were assessed.
Results: Differences (mean±1SD) were observed between low and high metabolically active regions: average BF (ml/100ml/min) 52±33 vs. 68±39 ml/100ml/min (p=0.03), average BV (ml/100ml) was 6.6±4.4 vs. 9.3±6.0 (p=0.06), MTT 5.8±3.8 vs. 6.0±4.1 s (p=0.62) and PMB (ml/100ml/min) was 13±19 vs. 20±27 (p<0.01), respectively.
Conclusions: Regions that are metabolically active on the FDG-PET scan also show increased blood flow, volume and permeability indicating more vascularised tumour parts. Mean transit times for the contrast were not different. These findings yield the potential to use perfusion imaging for characterization of vasculature in staging and follow-up of NSCLC patients scheduled for multi-modality therapy.

OC-0149

Non-invasive imaging of hypoxia with [18F]HX4 PET in NSCLC patients.

C.M.L. Zegers[1], W. van Elmpt[1], H. Sharifi[1], B. Reymen[1], M.C. Öllers[1], J. Eriksson[2], R. Wierts[3], F.M. Mottaghy[3], D. De Ruysscher[1], P. Lambin[1]
[1]*Department of Radiation Oncology (MAASTRO), Maastricht University Medical Centre, Maastricht, The Netherlands*
[2]*Departments of Nuclear Medicine and PET Research, VU University Medical Centre, Amsterdam, The Netherlands*
[3]*Department of Nuclear Medicine, Maastricht University Medical Centre, Maastricht, The Netherlands*

Purpose/Objective: Tumour hypoxia is an important marker of cancer prognosis, being associated with aggressive growth, metastasis and resistance to anticancer therapy. Imaging of tumour hypoxia could help to select patients for anti-hypoxia therapy and/or for a radiation boost to the hypoxic tumour regions. Pre-clinical data and phase I human trials have shown that [^{18}F]HX4 is a novel promising Positron Emission Tomography (PET) tracer for the evaluation of tumour hypoxia. The aims of the study were to evaluate the [^{18}F]HX4 uptake, the optimal imaging time-point after injection and the spatiotemporal stability in NSCLC patients.
Materials and Methods: 13 NSCLC patients (stage IIB-IV) included in 2 clinical trials (NCT01024829 and NCT01210378) were imaged on a PET/CT scanner using the hypoxia tracer: [^{18}F]HX4. 413±71 MBq of [^{18}F]HX4 was injected intravenously and at 2 and 4 hours p.i. PET acquisitions (30 min static) were acquired. SUV_{max} and SUV_{mean} were extracted from the gross tumour volumes (GTVs) and aortic arch to calculate tumour-to-blood ratios (TBR). The Wilcoxon signed rank test was used to determine significant differences in uptake between 2h and 4h post injection (p.i.) The tumour hypoxic fraction (HF), defined as the fraction of the GTV with a TBR>1.4, was determined for all lesions (i.e. primary tumour and lymph nodes). To evaluate the spatiotemporal stability, images acquired at 2h and 4h p.i. were rigidly registered and a voxelwise comparison of the [^{18}F]HX4 uptake was made, expressed as a Pearson correlation coefficient.
Results: Analysis of the first 13 NSCLC patients (9 male, 4 female, age: 62±12 y), indicated significant uptake (TBR>1.4) in 18/25 target lesions (13 primary tumours and 12 lymph nodes) with an average HF of 20±21% (range: 0.2-71%) at 4h p.i.. 85% (11/13) of the primary tumours and 58% (7/12) of the involved lymph nodes were hypoxic. There was no correlation between the GTV and HF (R=0.25, P=0.24). Within the 18 hypoxic lesions, the average tumour SUVmax decreased significantly (P=0.004) from 2h (1.4±0.4) to 4h p.i. (1.2±0.4). However, due to clearance of [^{18}F]HX4 in the blood, the TBR increased significantly (P<0.001) between 2h and 4h p.i. from 1.6±0.3 to 2.0±0.5 (see figure). The heterogeneous [^{18}F]HX4 uptake pattern at 2h and 4h p.i. showed a strong correlation (R=0.76±0.09, range: 0.58-0.94).

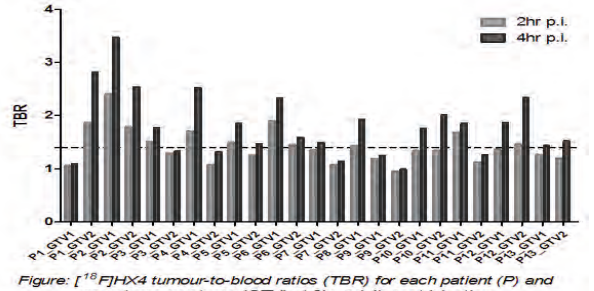

Figure: [^{18}F]HX4 tumour-to-blood ratios (TBR) for each patient (P) and gross tumour volume (GTV) at 2h and 4h post injection.

Conclusions: Significant hypoxia was observed in 72% of the NSCLC target lesions (85% of primary tumours and 58% of the involved lymph nodes). The heterogeneous [^{18}F]HX4 uptake pattern was stable between 2h and 4h p.i., however the TBR increased over time,